Journal of Pain Research

Dovepress
open access to scientific and medical research

Open Access Full Text Article

ORIGINAL RESEARCH

Electroacupuncture Alleviates Dry Eye Ocular Pain Through TNF-α Mediated ERK1/2/P2X$_3$R Signaling Pathway in SD Rats

Mi-Mi Wan[1,*], Tuo Jin[2,*], Zhang-Yitian Fu[1], Si-Hua Lai[1], Wei-Ping Gao[1]

[1]Department of Ophthalmology, Affiliated Hospital of Nanjing University of Chinese Medicine, Nanjing, People's Republic of China; [2]Department of Ophthalmology, Kunshan Hospital of Chinese Medicine, Suzhou, People's Republic of China

*These authors contributed equally to this work

Correspondence: Wei-Ping Gao, Department of Ophthalmology, Affiliated Hospital of Nanjing University of Chinese Medicine, No. 155 Hanzhong Road, Qinhuai District, Nanjing, Jiangsu, People's Republic of China, Tel +86 13057671767, Email 260790@njucm.edu.cn

Purpose: This study aimed to examine electroacupuncture's influence on ocular pain and its potential modulation of the TNF-α mediated ERK1/2/P2X$_3$R signaling pathway in dry eye-induced rat models.

Methods: Male Sprague–Dawley rats with induced dry eye, achieved through extraorbital lacrimal gland removal, were treated with electroacupuncture. Comprehensive metrics such as the corneal mechanical perception threshold, palpebral fissure height, eyeblink frequency, eye wiping duration, behavioral changes in the open field test, and the forced swimming test were employed. Additionally, morphological changes in microglia and neurons were observed. Expression patterns of key markers, TNF-α, TNFR1, p-ERK1/2, and P2X$_3$R, in the trigeminal ganglion (TG) and spinal trigeminal nucleus caudalis (SpVc) regions, were studied with etanercept serving as a control to decipher the biochemistry of electroacupuncture's therapeutic effects.

Results: Electroacupuncture treatment demonstrated a notable decrease in the corneal mechanical perception threshold, improvement in palpebral fissure height, and significant reductions in both eyeblink frequency and eye wiping duration. Moreover, it exhibited a promising role in anxiety alleviation. Notably, the technique effectively diminished ocular pain by curbing microglial and neuronal activation in the TG and SpVc regions. Furthermore, it potently downregulated TNF-α, TNFR1, p-ERK1/2, and P2X$_3$R expression within these regions.

Conclusion: Electroacupuncture attenuated damage to sensory nerve pathways, reduced pain, and eased anxiety in dry eye-afflicted rats. The findings suggest a crucial role of TNF-α mediated ERK1/2/P2X$_3$R signaling pathway inhibition by electroacupuncture in these benefits.

Keywords: electroacupuncture, dry eye, ocular pain, TNF-α, ERK1/2/P2X$_3$R signaling pathway

Introduction

In 2017, TFOS DEWS II posited that the symptoms of discomfort stemming from dry eye (DE) can be categorized as a distinct type of pain.[1] It is a prevailing theory that neuropathic pain mechanisms predominantly drive DE ocular pain, manifested as itching, burning, photosensitivity, dryness, a gritty sensation, and stinging.[2] This involves both peripheral and central sensory nerve pathways in symptom origination and persistence. Crucially, peripheral and central sensitization are foundational in the perpetuation of chronic pain perception.[3]

A decline in tear secretion, variations in tear film osmotic pressure, and corneal epithelial defects resultant from DE can stimulate the corneal nociceptors in the trigeminal ganglion, then relay nociceptive stimulus signals via the nasociliary branch of the trigeminal ganglion (TG) to the caudal subnucleus of the spinal trigeminal nucleus caudalis (SpVc). This sequence culminates in the impulses reaching the sensory region of the cerebral cortex through the thalamus,[4,5] prompting the sensation of pain. Prolonged DE contributes to sustained pathological excitement of the trigeminal sensory conduction trajectory. This

Received: 14 September 2023
Accepted: 4 December 2023
Published: 12 December 2023

activity subsequently ignites microglia and triggers the release of a plethora of inflammatory factors.[6] Such inflammation not only inflicts neuronal damage[7] but also incites sensitization in both surrounding and central nervous systems.[8] This cascade establishes the pathological foundation of DE ocular pain.

Electroacupuncture (EA) has garnered attention over the years as a potential therapeutic avenue for DE.[9,10] Noteworthy is its capacity to modulate various cell signal transduction pathways, mitigating neuroinflammation.[11] It also stands out for effectively ameliorating pain, circumventing the adverse consequences—such as addiction, immune compromise, and gastrointestinal harm—often affiliated with analgesics.[12] This significantly elevates the life quality of those grappling with pain. Notably, TNF-α, emblematic of inflammation, is intricately linked to pain's evolution. Preliminary research, grounded in animal pain models, postulates that EA can influence the expression of TNF-α, p-ERK1/2, and $P2X_3R$, leading to pain relief.[13–15] Thus, this investigation seeks to elucidate the role of the TNF-α mediated ERK1/2/$P2X_3R$ signaling pathway and discern the analgesic workings of EA in model rats subjected to DE ocular pain. This inquiry aims to bolster the empirical basis for employing EA in DE ocular pain treatment.

Materials and Methods

Animals

Healthy male Sprague Dawley rats weighing 300–330g (license number: SCXK (Lu) 2019–0003, Jinan Pengyue Experimental Animal Breeding Co., Ltd) were housed in the Basic Pharmacology Laboratory of the Affiliated Hospital of Nanjing University of Chinese Medicine, with five animals per cage, allowing them to freely drink and eat. The rats were kept in a controlled environment with a 12-hour light-dark alternating cycle, at a temperature of 21 ± 2° C and a relative humidity of 40–60%. The animal experiments conformed to the relevant provisions of the national experimental animal welfare ethics and were approved by the Ethics Committee of the Affiliated Hospital of Nanjing University of Chinese Medicine (batch number: 2021 DW-02-02). All experimental protocols were in accordance with the Guiding Opinions on Treating Experimental Animals issued by the Ministry of Science and Technology of the People's Republic of China.

Establishment of DE Ocular Pain Rat Models

The rats were anesthetized using isoflurane (flow rate of 3 L/min) using an animal anesthesia machine (model number: ABS, serial number: Y655650326, Shanghai Yuyan Scientific Instrument Co., Ltd., China). The surgical area was skin prepared and disinfected, and a 0.5 cm transverse incision was made approximately 0.8 cm vertically downward from the middle of the line connecting the rat's outer canthus and the lower opening of the ipsilateral external auditory canal. The muscle capsule was dissected, and the extraorbital lacrimal gland was completely removed. The wound was rinsed with physiological saline, sutured, and lidocaine hydrochloride gel was applied to alleviate pain.[16]

Electroacupuncture

The disposable sterile acupuncture needles (0.18 mm * 13 mm, Huatuo Medical Instruments Co., Ltd., China) were inserted into the bilateral "Jingming" (BL1), "Cuanzhu" (BL2), "Sizhukong" (SJ23), "Tongziliao" (GB1) and "Taiyang" (EX-HN5) of the rats, following the guidelines for experimental acupuncture and moxibustion.[17] Then, a pair of electrodes from an EA instrument (SDZ-II B-type, Huatuo Medical Instruments Co., Ltd., China) were connected to the ipsilateral "Cuanzhu" and "Taiyang", using dilatational wave with a frequency of 4 Hz/20 Hz, pulse width of 0.2ms, output intensity of 1mA, and EA for 15 minutes, once a day.[9]

Experimental Design

In experiment 1, a total of 60 rats were randomly divided into six groups: blank (n=10), surgery (n=10), sham surgery (n=10), EA (n=10), sham EA (n=10), and pranoprofen (n=10) groups. On the 0th day, surgery was performed to establish the model of DE ocular pain. The sham surgery group had the extraorbital lacrimal gland exposed, and the incision was sutured. The interventions began on the 15th day, lasting for 14 days in the EA group, sham EA group, and pranoprofen group. The rats in the EA group were treated with EA for 15 minutes once daily. The rats in the sham EA group were treated with blunt head acupuncture for 15 minutes each day.[18] The rats in the pranoprofen group were treated with

pranoprofen eye drops three times a day at 8:00, 14:00, and 17:00, with one drop per eye. In experiment 2, 28 rats were randomly divided into the following groups: surgery+NS (n=7), EA+NS (n=7), etanercept (n=7), and EA+etanercept (n=7) groups. On day 0, extraorbital lacrimal gland removed surgery was performed in each group to establish a model of DE ocular pain. The surgery+NS group received intraperitoneal injection of 0.06 mL/kg normal saline (NS) on days 15 and 20 of the experiment. Based on the intervention method for the EA group in experiment 1, the EA+NS group received additional intraperitoneal injections of 0.06 mL/kg of NS on the 15th and 20th days of the experiment. The etanercept group was intraperitoneally injected with etanercept at a dose of 0.06 mL/kg (specification: 0.47 mL: 25 mg, batch number: FR7452, Pfizer Biopharmaceutical Company, USA)[19] on the 15th and 20th days of the experiment. Similarly, based on the intervention method used in experiment 1, the EA+etanercept group received additional intraperitoneal injections of etanercept at a dose of 0.06 mL/kg on the 15th and 20th days of the experiment. The same tester conducted all tests for all time periods, and unaware of the grouping of the rats. On the both of the 29th day of the two experiment, all rats were euthanized, and tissues were collected. (Figure 1a and 1b)

Detection Indicators and Methods

Corneal Mechanical Sensitivity

The Cochet-Bonnet corneal perception instrument measured the corneal mechanical perception threshold in rats, which is inversely related to corneal mechanical sensitivity (CTT). The tester gently touched the central area of the rat's cornea vertically using the tip of the nylon thread which was adjusted to a total length of 60 mm. The length of the thread at which two out of three repeated stimuli triggered a blinking reflex represented the mechanical perception threshold of the rat's cornea. The length of the nylon thread (5 mm) was gradually reduced, and the procedure was repeated until the rat exhibited a blink reflex. The results were respectively measured and recorded on days 0, 7, 14, 21, and 28.

Palpebral Fissure Height

The binocular palpebral fissure heights of the rats were measured using a film ruler with an accuracy of 0.5 mm. The height of the eyelid fissure was defined as the distance between the edges of the upper and lower eyelids passing through the center of the cornea and perpendicular to the line connecting the inner and outer canthus. The results were respectively measured and recorded on days 0, 7, 14, 21, and 28.

Eyeblinks Frequency

After 15 min of acclimatization, binocular eyeblink counts of the rats were observed within 5 minutes in a transparent box.[20] The results were respectively measured and recorded on days 0, 7, 14, 21, and 28.

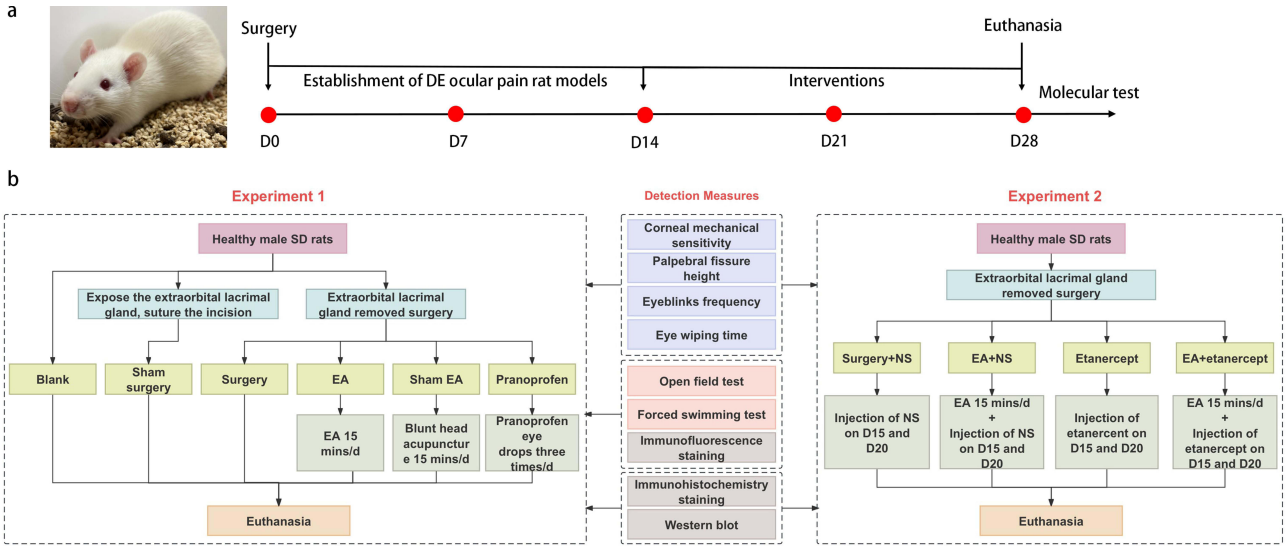

Figure 1 (**a**) Timeline of the experiment; (**b**) Flowchart of Experiment1 and 2.

Eye Wiping Time

Rats were placed in a transparent box and allowed to move freely. 40 μL of 1 M NaCl solution was dropped into binoculus, and the total time they spent wiping their eyes within 3 minutes was recorded. Subsequently, the eyes were rinsed with physiological saline, and the rats were treated with 40 μL of 2.5 M NaCl solution in both eyes, repeating the same procedure as before.[21] The results of the experiments were respectively measured and recorded on days 14 and 28.

Open Field Test

The testing area consisted of an open-field experimental box (model: XR-XZ301, Shanghai Xinruan Information Technology Co., Ltd., China) measuring 100×100 × 40 cm and a camera placed 2 m above the center. A data acquisition system (SuperMaze software, Shanghai Xinruan Information Technology Co., Ltd., China) was used to record the data captured by the camera and perform image processing and analysis. Each rat was placed in the center of the box, and its video signals of activity were collected and recorded within 5 min. The total distance traveled by the rat was then analyzed. The results of the experiments were measured and recorded on days 0, 14, and 28.

Forced Swimming Test

The experimental device (model: XR-XQ202, Shanghai Xinruan Information Technology Co., Ltd., China) was a transparent resin bucket with a height of 50 cm and a diameter of 40 cm. Each rat was placed in water with a height of 35 cm, maintained at a temperature of 22–26°C. The rats were forced to swim for 5 min, and the time at which they remained motionless was recorded and analyzed by data collection system (SuperMaze software). The results of the experiments were measured and recorded on days 0, 14, and 28.

Immunofluorescence Staining

The PFA fixed trigeminal ganglia and medulla oblongata were dehydrated, embedded, sliced, dewaxed and hydrated. After antigen repair, the slices were blocked for 30min. For double-labeling immunofluorescence of $P2X_3R$ and NeuN, the slices were incubated with NeuN (1:2000; GB11138, Servicebio, China) at 4°C overnight. On the second day, horseradish peroxidase-labeled goat anti-rabbit IgG (1:300; GB23303, Servicebio, China) was added to the slices and incubated for 50 min. After washing, FITC Tyramide (1:500; G1222, Servicebio, China) was added, which were then incubated for 10 min. After the second antigen repair, $P2X_3R$ (1:200; bs-4249R, Bioss, China) was added to slices for overnight incubation at 4°C. CY3 labeled goat anti-rabbit IgG (1:300; GB21303, Servicebio, China) was added to the slices the next day, and the slices were incubated for 50 min. For double-labeling heterologous immunofluorescence of TNF-α and Iba1, the slices were incubated with a mixture of TNF-α (1:2000; 60,291-1-Ig, Proteintech, China) and Iba1 (1:500; GB11105, Servicebio, China) overnight at 4°C. The following day, CY3 labeled goat anti-mouse IgG (as described above) and Alexa Fluor 488 labeled goat anti-rabbit IgG (1:400, GB25303, Servicebio, China) were added and incubated for 50 min. For immunofluorescence of c-fos, the slices were incubated with c-fos (1:200; GB1069, Servicebio, China) overnight at 4°C. CY3 labeled goat anti-rabbit IgG (as described above) was added to the slices the next day, and the slices were incubated for 50 min. Images were captured and analyzed under a fluorescence microscope (Nikon Eclipse C1, Japan).

Immunohistochemistry Staining

After prepared slices were rinsed and blocked, TNF-α (1:2000; 60,291 1-Ig, Proteintech, China), TNFR1 (1:2000; 60,192 1-Ig, Proteintech, China), p-ERK1/2 (1:2000; 28,733 1-AP, Proteintech, China), and $P2X_3R$ (1:100; bs-4249R, Bioss, China) were respectively added to the slices for overnight incubation at 4°C. The corresponding secondary antibodies (1:500, G1213-100UL; G1214-100UL, Servicebio, China) were added to the slices and incubated for 50 minutes the next day. The color was developed using DAB, followed by staining with hematoxylin and rinsing. Images were observed under a microscope (Nikon Eclipse E200, Japan). The ImageJ software was used for image analysis to calculate the average optical density.

Western Blot

The protein extracted from TG and SpVc were quantified using the bicinchoninic acid method. Equivalent protein samples were wet-transferred to a PVDF membrane after electrophoresis. After blocked for 2h, primary antibodies

including TNF-α (1:1000; 60,291-1-Ig, Proteintech, China), TNFR1 (1:1000; 60,192-1-Ig, Proteintech, China), p-ERK1/2 (1:1000; 28,733-1-AP, Proteintech, China) and $P2X_3R$ (1:1000; bs-4249R, Bioss, China) were added to the PVDF membranes and incubated overnight at 4°C. The following day, secondary antibodies (1:3000; # S0001, # S0002, Affinity, USA) were added to the membranes and incubated for 2 hours. The membranes were exposed by chemiluminescence detection. After proteins removed from the membranes by antibody elution, subsequent re-exposure was carried out using GAPDH (1:5000; 10,494-1-AP, Proteintech, China) for detection. Grayscale values of the bands were analyzed using ImageJ image analysis software, and the ratio of the target protein to GAPDH represented the relative expression level.

Statistical Analysis

SPSS software (version 26.0) was used for data analysis and processing. Data are expressed as the mean ± standard error (x± SEM). One-way ANOVA was used for comparisons between each group, and Two-way ANOVA was used for multiple comparisons between each group of different times. Nonparametric tests were selected if the data did not conform to a normal distribution or homogeneity of variance. $P<0.05$ indicates the difference in comparison, at $P<0.01$ represents the significant difference.

Results

EA Efficaciously Alleviates Pain Symptoms in DE Ocular Pain Model Rats

To assess the impact of EA on the symptoms of DE ocular pain in model rats, we examined both the physical manifestations on the ocular surface and associated pain behaviors. Our observations suggest that EA notably diminishes corneal mechanical sensitivity (Figure 2a), augments eyelid fissure height (Figure 2c), curtails blink frequency (Figure 2e) and eye wiping duration (Figure 2g and h), extends the total distance traveled in the open field test (Figure 2k and 2m), and reduces idle time in the forced swimming test (Figure 2l) among DE ocular pain model rats. For comparative efficacy, we selected etanercept as an intervention. The outcomes revealed that the therapeutic effects of EA were analogous to those of etanercept in terms of metrics like corneal mechanical sensitivity (Figure 2b), palpebral fissure heights (Figure 2d), blink frequency (Figure 2f), and eye wiping duration (Figure 2I and j).

EA Significantly Inhibits Microglial and Neuronal Activation in TG and SpVc of DE Ocular Pain Model Rats

Our objective was to identify specific sites of action for EA in the treatment of DE ocular pain. Examination of cells within the TG and SpVc revealed heightened activation of microglia and neurons in the DE ocular pain model rats. EA treatment substantially curtailed this activation, an outcome not achieved with pranoprofen (Figure 3e–j). Concurrently, positive expression markers for TNF-α and $P2X_3R$ were identified on microglia and neurons within TG and SpVc of the DE ocular pain model rats (Figure 3a–d). This observation may substantiate subsequent analyses regarding the involvement of the TNF-α mediated ERK1/2/$P2X_3R$ signaling pathway in the regulation of DE ocular pain.

EA modulates Expression in the TNF-α Mediated ERK1/2/$P2X_3R$ Signaling Pathway in TG and SpVc of DE Ocular Pain Model Rats

To delve deeper into the molecular underpinnings of EA's efficacy in treating DE ocular pain, we studied the expression patterns of TNF-α, TNFR1, p-ERK1/2, and $P2X_3R$ within TG and SpVc. TNF-α, when released by microglia, serves as an external inflammatory stimulus, binding to the TNFR1 on sensory neurons' surfaces. Our findings highlight that EA can markedly diminish TNF-α levels, significantly attenuating its affinity for TNFR1 and consequently stymieing the downstream phosphorylation activity of ERK1/2. The presence of $P2X_3R$ on neuronal surfaces perpetuates injury signals. However, acupuncture can considerably mitigate the release of $P2X_3R$ by repressing ERK1/2 expression, thereby obstructing pain signals from accessing the brain via sensory nerves (Figure 4a–e, k–n and Figure 5a–e, k–n). When juxtaposed with etanercept, we noted that the TNF-α expression in the etanercept group was substantially muted

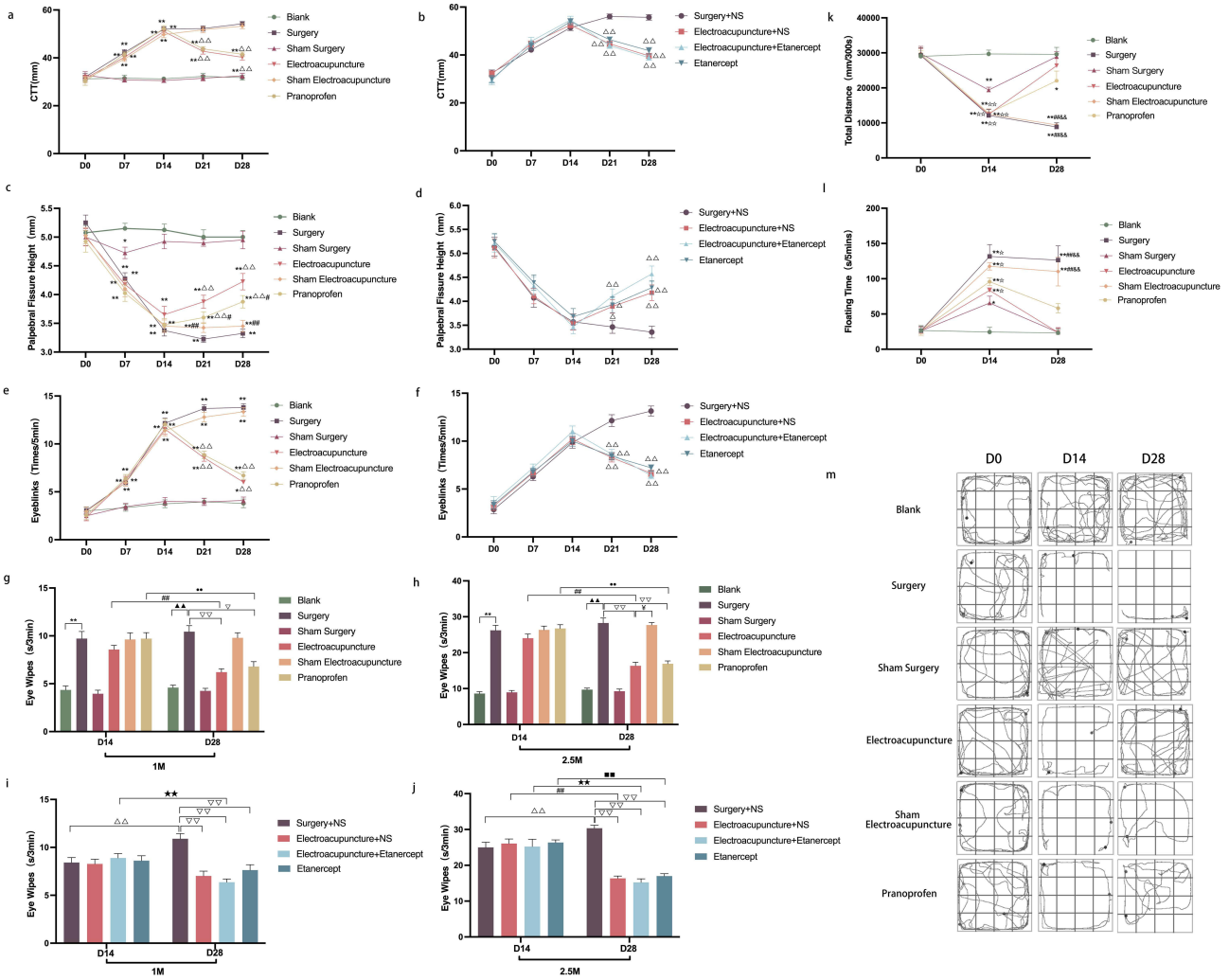

Figure 2 (**a** and **b**) Line comparison of the corneal mechanical perception thresholds of rats; (**c** and **d**) Line comparison of the height of eyelid fissures in each group of rats; (**e** and **f**) Line comparison of the blink frequency of each group of rats; Data are expressed as mean ± standard error, n=20 (eyes) in experiment 1 (**a, c** and **e**), n=14 (eyes) in experiment 2 (**b, d** and **f**). *P<0.05, **P<0.01 versus blank group; ΔP<0.05, ΔΔP<0.01 versus surgery group (surgery+NS group); $^{\#}$P<0.05, $^{\#\#}$P<0.01 versus EA group. (**g–j**) Comparison of the eye wiping time of each group of rats under the stimulation of 1 M and 2.5 M NaCl solution; Data are expressed as mean ± standard error, n=10 (eyes) in experiment 1 (**g** and **h**), n=7 (eyes) in experiment 2 (**I** and **j**). **P<0.01 versus blank group on D14; ΔΔP<0.01 versus surgery group (surgery+NS group) on D14; $^{\#\#}$P<0.01 versus EA group (EA+NS group) on D14; ●●P<0.01 versus pranoprofen group on D14; ★★P<0.01 versus EA+etanercept group on D14; ■■P<0.01 versus etanercept group on D14. ▲P<0.05, ▲▲P<0.01 versus blank group on D28; ▽P<0.05, ▽▽P<0.01 versus surgery group (surgery+NS group) on D28; ¥P<0.05 versus EA group (EA+NS group) on D28. (**k**) The line comparison chart of the total distance of open field tests in each group on D0, D14 and D28; (**l**) The line comparison of the floating time of forced swimming teats in each group on D0, D14 and D28; (**m**) Trajectory map of autonomous activity exploration behavior of rats in open field tests on D0, D14 and D28; Data are expressed as mean ± standard error, n=4. *P<0.05, **P<0.01 versus blank group; ☆☆P<0.01 versus sham surgery group; $^{\#\#}$P<0.01 versus EA group; $^{\&\&}$P<0.01 versus pranoprofen group.

compared to the EA+NS group. However, levels of TNFR1, p-ERK1/2, and $P2X_3R$ in the etanercept group considerably eclipsed those observed in the EA+NS cohort (Figure 4f–j, o–r and Figure 5f–j, o–r).

Discussion

Our research on DE ocular pain treatment utilized EA, drawing from the principles of traditional Chinese medicine and addressing the contemporary scientific challenges associated with DE ocular pain. We determined that EA exhibited significant therapeutic effects on variables such as corneal mechanical sensitivity, eyelid fissure height, blink frequency, eye-wiping duration, anxiety, and depression. These effects collectively mitigated the symptoms of DE ocular pain in our rat models. We postulate that the mechanisms underpinning these results involve EA's ability to diminish the activation of neurons and microglia in TG and SpVc. Furthermore, EA appears to modulate the TNF-α-mediated ERK1/2/$P2X_3$

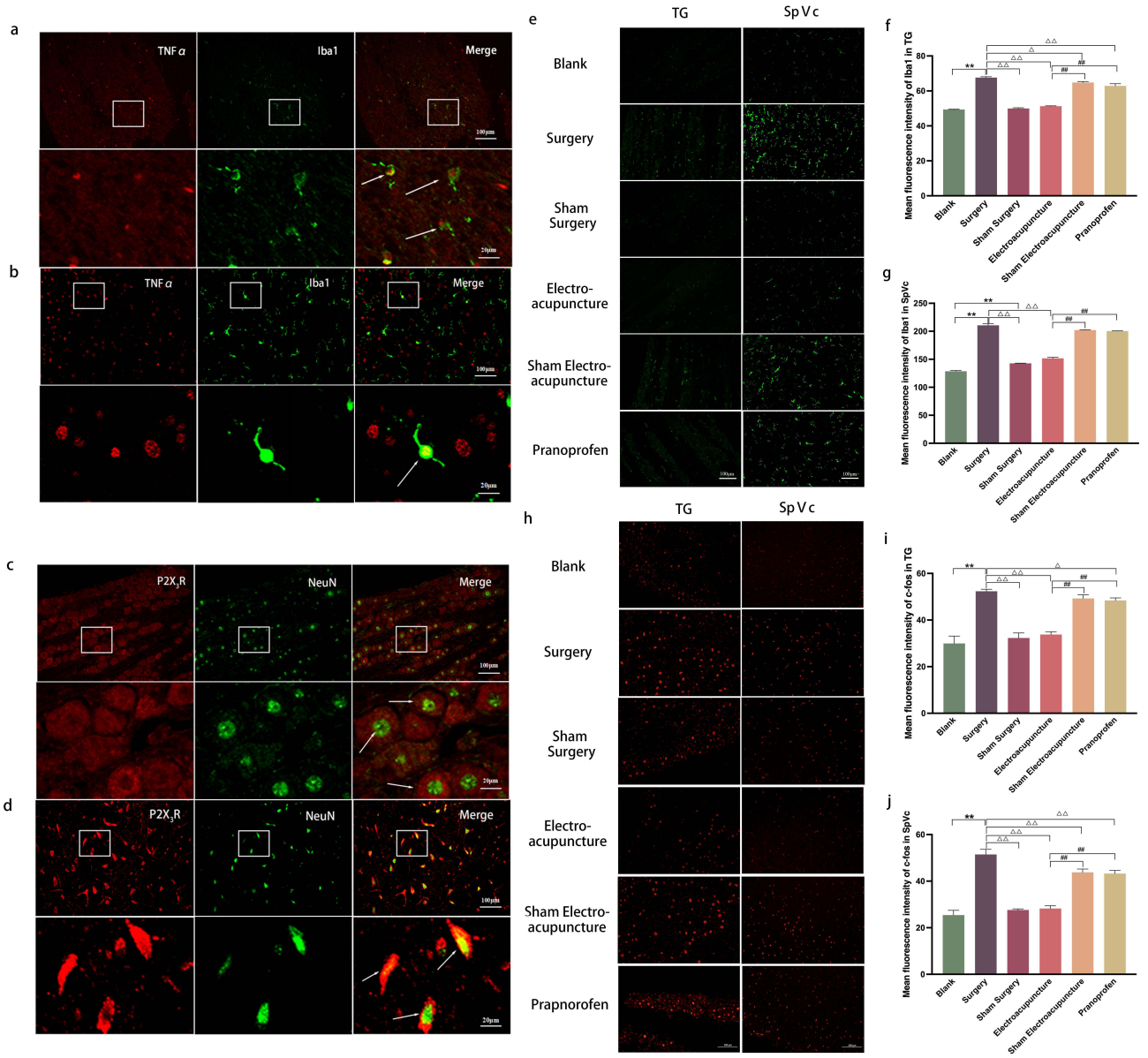

Figure 3 (**a** and **b**) Co-localization of TNF-α (red) with Iba1 (green) in TG and SpVc observed through immunohistochemical fluorescence; Activation of Iba1 was observed, with an increase in microglia cell body and shorter protuberance; The morphology of microglia became round or rod-shaped. The cells marked by the white arrow indicate cells where TNF-α co-localizes with Iba1; (**c** and **d**) Co-localization of $P2X_3R$ (red) and NeuN (green) in TG and SpVc observed through immunohistochemical fluorescence; $P2X_3$ R was widely expressed on neurons; The cells marked by the white arrow represent the co-localized cells of $P2X_3R$ and NeuN; The enlarged images correspond to the magnified views of the cells in the a-d diagrams, respectively; Scale bar = 100 μm; Enlarged image scale bar = 20 μm. (**e** and **h**) Immunohistochemical fluorescence of Iba1/c-fos in TG and SpVc of rats in each group; Scale bar = 100 μm. (**f** and **i**) Histogram of the average fluorescence intensity of Iba1/c-fos in the TG of rats in each group. (**g** and **j**) Histogram of the average fluorescence intensity of Iba1/c-fos in SpVc of rats in each group. Data are expressed as mean ± standard error, n=3. *P<0.05, **P<0.01 versus blank group; ΔP<0.05, ΔΔP<0.01 versus surgery group; $^{\#}$P<0.05, $^{\#\#}$P<0.01 versus EA group.

R signaling pathway in these regions, inhibit inflammatory factor release from microglia to neurons, attenuate the activation of the purinergic receptor, and ultimately alleviate ocular pain in DE model rats.

In our experimental design, we surgically removed the extraorbital lacrimal gland from male SD rats. Subsequent observations revealed a series of ocular pain symptoms, specifically aligned with the reports of Fakih, Rahman, and Meng.[22–24] Their prior studies reported that removing the infraorbital and/or extraorbital lacrimal glands in animals produces a range of effects, including enhanced mechanical sensitivity of the corneas, augmented eye-wiping and blinking responses to hypertonic saline stimuli, increased spontaneous ciliary nerve fiber electrical activity, heightened orbicularis oculi muscle activity, and the sensitization of eye reflex neurons, especially in various regions of the spinal

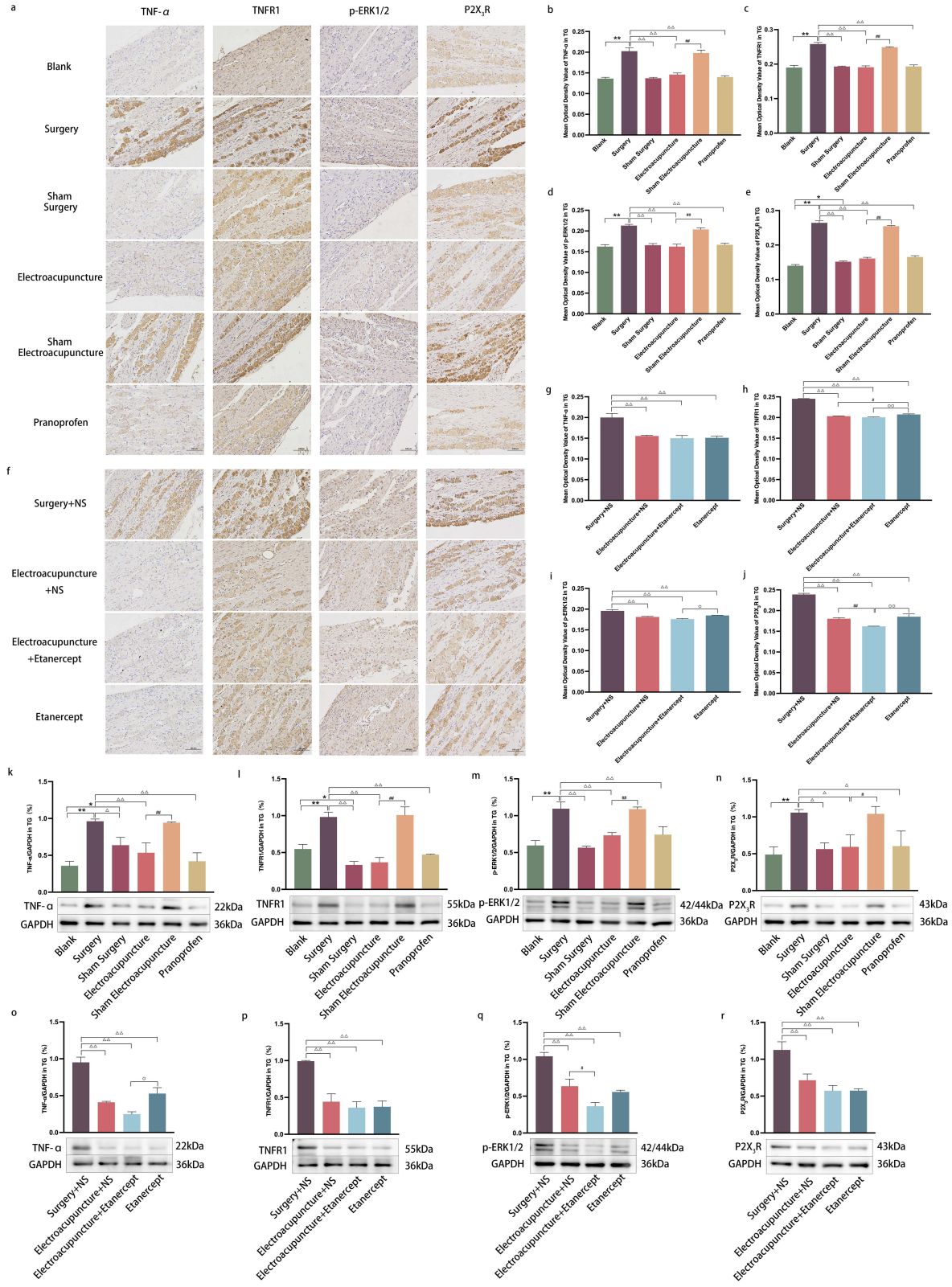

Figure 4 (**a** and **f**) The stained areas (brown) respectively represents TNF-α, TNFR1, p-ERK1/2 and P2X$_3$R immunopositive cells of TG in experiment 1 and experiment 2; Scale bar = 100 μm; (**b–e** and **g–j**) Immunohistochemical semi-quantitative analysis (average optical density value) of TNF-α, TNFR1, p-ERK1/2 and P2X$_3$R in different groups of experiment 1 and experiment 2 in TG; Data are expressed as mean ± standard error, n=3; **P*<0.05, ***P*<0.01 versus blank group; Δ*P*<0.05, ΔΔ*P*<0.01 versus surgery group (surgery +NS group); #*P*<0.05, ##*P*<0.01 versus EA group (EA+NS group); ○*P*<0.05, ○○*P*<0.01 versus Etanercept group. (**k–r**) Protein expressions of TNF-α, TNFR1, p-ERK1/2 and P2X$_3$ R of TG by Western blot and semi-quantitative analysis in experiment 1 and experiment 2; Data are expressed as mean ± standard error, n=3; **P*<0.05, ***P*<0.01 versus blank group; Δ*P*<0.05, ΔΔ*P*<0.01 versus surgery group (surgery+NS group); #*P*<0.05, ##*P*<0.01 versus EA group (EA+NS group); ○*P*<0.05, ○○*P*<0.01 versus etanercept group.

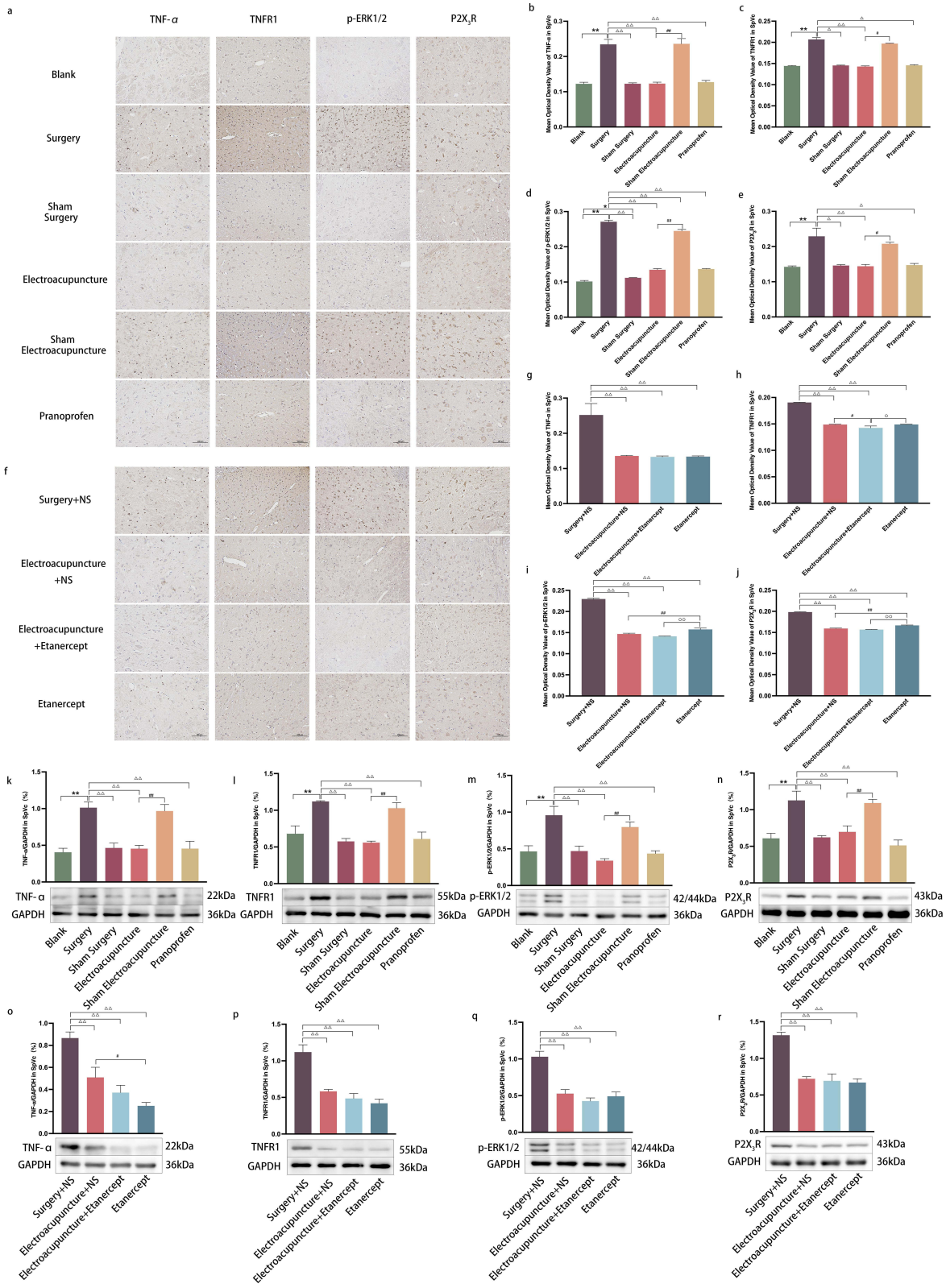

Figure 5 (**a** and **f**) The stained areas (brown) respectively represents TNF-α, TNFR1, p-ERK1/2 and P2X$_3$R immunopositive cells of SpVc in experiment 1 and experiment 2; Scale bar =100 μm; (**b–e** and **g–j**) Immunohistochemical semi-quantitative analysis (average optical density value) of TNF-α, TNFR1, p-ERK1/2 and P2X$_3$R in different groups of experiment 1 and experiment 2 in SpVc; Data are expressed as mean ± standard error, n=3; *P<0.05, **P<0.01 versus blank group; ΔP<0.05, ΔΔP<0.01 versus surgery group (surgery+NS group); $^{\#}$P<0.05, $^{\#\#}$P<0.01 versus EA group (EA+NS group); ○P<0.05, ○○P<0.01 versus etanercept group. (**k–r**) Protein expressions of TNF-α, TNFR1, p-ERK1/2 and P2X$_3$R of SpVc by Western blot and semi-quantitative analysis in experiment 1 and experiment 2; Data are expressed as mean ± standard error, n=3; **P<0.01 versus blank group; ΔΔP<0.01 versus surgery group (surgery+NS group); $^{\#}$P<0.05, $^{\#\#}$P<0.01 versus EA group (EA+NS group).

trigeminal subnucleus caudalis. Given that model animals cannot communicate their sensations, these objective markers offer invaluable insights into the efficacy of our model preparations. Our data further suggests that the lacrimal gland resection DE model holds promise as a reliable framework for investigating DE ocular pain treatments and might also shed light on the pathophysiological underpinnings of DE ocular pain.

Additionally, we conducted a semi-quantitative analysis of Iba1 and c-fos expression in TG and SpVc. Elevated expressions of Iba1 and c-fos within the surgical cohort implied heightened microglia and neuron activation. Prior research by Galor and Fakih corroborates our findings, highlighting that in chronic DE model animals, the neural tissue in TG and SpVc undergoes pathological shifts, predominantly excessive neuron and microglia activation.[16,25] Microglia, pivotal to nerve damage and chronic pain perpetuation.[26] Zhao discerned that in DE animal models, sensory nerve tissue microglia undergo rapid activation, resulting in cell body enlargement and dendritic thickening.[27] This morphological transformation mirrors our own observations. The subsequent release of inflammatory mediators by these activated microglia heightens neuronal excitatory discharges, which is considered might contribute to both peripheral and central sensitization processes.[28] As a result, activated microglia amplify the sensory transmission pathway's excitability, leading to bodily pain.[7] This framework aptly elucidates our observed c-fos expression surge and provides a rationale for the resultant ocular pain, aligning with Kikuchi's perspectives.[29]

The suppression of TNF-α has been demonstrated to alleviate pain and hyperalgesia in animal models related to pain.[30,31] While some studies that focused on DE treatment using EA with a focus on TNF-α, our research posits that the therapeutic mechanism of EA for DE ocular pain might mirror that of TNF-α antagonism. This is accomplished by preventing TNF-α from associating with TNFR1, an assertion that aligns with previous research findings.[32,33] Moreover, the therapeutic potency of EA in pain mitigation is underscored by its ability to curb $P2X_3R$ expression.[34,35] Upon $P2X_3R$ activation, neurons generate spontaneous excitatory postsynaptic currents, which subsequently govern the release of various pain-inducing neurotransmitters, culminating in pain sensitization.[36] Our findings indicate that EA mitigates pain perception by diminishing $P2X_3R$ functionality on neuronal surfaces. Furthermore, our observations indicate ERK1/2's role in DE pain onset. Recognized as a pivotal molecule in pain transmission, ERK1/2 has emerged as a promising target for pain intervention.[37] Activated via phosphorylation, ERK1/2 orchestrate a cascade of changes in the expression of inflammatory and pain-related cytokines.[38] It appears that EA can modulate ERK1/2 expression, thereby counteracting ocular pain. Nonetheless, the literature currently offers limited insights into ERK1/2's involvement in DE progression and EA's influence on it.

Our research introduces a novel proposition that EA's therapeutic approach to DE ocular pain operates by inhibiting the binding of TNF-α to TNFR1 and subsequently decreasing the expression of downstream p-ERK1/2 and $P2X_3R$. While the analgesic properties of pranoprofen eye drops parallel those of EA, a distinction lies in EA's ability to ameliorate the activation of both microglia and neurons, a capability absent in pranoprofen eye drops. These findings could pave the way for a refreshed theoretical framework supporting the application of EA in treating DE.

Furthermore, our study illuminates DE ocular pain's potential to intensify emotional disturbances, particularly anxiety and depression,[39] which could be discerned by examining animals' instinctive behaviors.[40,41] In assessing the behaviors of DE ocular pain-afflicted rats through open field and forced swimming tests, we discerned that DE could instigate depression-like symptoms. Encouragingly, EA demonstrated potential in alleviating these symptoms, a relief we hypothesize is linked to its analgesic properties. EA's capacity to mitigate DE ocular pain-induced depression remains a promising avenue for future behavioral studies. Besides, due to the limitation of objective observation indicators for ocular pain animal models, we plan to further observe the performance of rats in dry eye ocular pain through neuroelectrophysiological methods.

Building upon the foundational research of our group, we adopted a singular EA treatment protocol for intervention. Our future endeavors will delve into the potential varying therapeutic efficacies of different EA treatment frequencies or intensities on DE ocular pain.

Notably, glial cells play a pivotal role in pain inception and progression.[6] Our findings affirm that EA suppresses microglial activation and subsequent inflammatory cytokine release.[42] Beyond microglia, the analgesic and neuromodulatory prowess of EA might extend to other cells, such as astrocytes and oligodendrocytes.[43,44] However, the literature remains sparse regarding the modulatory effects of EA on the entire glial cell family. As such, we advocate for comprehensive research to ascertain the potential of EA in modulating a broader range of cells, including glial cells, when addressing DE ocular pain.

Conclusion

This study highlights the potential of electroacupuncture in mitigating ocular pain within a dry eye rat model. Our findings unravel the underlying TNF-α mediated ERK1/2/$P2X_3R$ signaling pathway, offering clinicians a novel theoretical foundation for dry eye treatment using acupuncture.

Data Sharing Statement

The data used to support the results of this study can be obtained from the corresponding author upon reasonable request.

Acknowledgments

Mi-Mi Wan and Tuo Jin are co-first authors for this study. We would like to extend our gratitude to M.D. Qin-Mei Sun from the Shanghai University of Traditional Chinese Medicine for her invaluable suggestions on manuscript composition. Additionally, we are thankful to Qi-Yu Zhao from the USA for his linguistic edits and enhancements.

Funding

This study was supported by the National Natural Science Foundation of China [No. 82074526; Nanjing, China] and the Postgraduate Research & Practice Innovation Program of Jiangsu Province [No. KYCX23_2138; Nanjing, China].

Disclosure

No potential conflict of interest was reported by the authors.

References

1. Belmonte C, Nichols JJ, Cox SM, et al. TFOS DEWS II pain and sensation report. *Ocul Surf*. 2017;15(3):404–437. doi:10.1016/j.jtos.2017.05.002
2. Melik Parsadaniantz S, Rostène W, Baudouin C, et al. Understanding chronic ocular pain. *Biol Aujourdhui*. 2018;212(1–2):1–11. doi:10.1051/jbio/2018017
3. Kim J, Yoon HJ, You IC, et al. Clinical characteristics of dry eye with ocular neuropathic pain features: comparison according to the types of sensitization based on the ocular pain assessment survey. *BMC Ophthalmol*. 2020;20(1):455. doi:10.1186/s12886-020-01733-1
4. Moulton EA, Borsook D. C-fiber assays in the cornea vs. Skin. *Brain Sci*. 2019;9:11. doi:10.3390/brainsci9110320
5. Bernier LP, Ase AR, Séguéla P. P2X receptor channels in chronic pain pathways. *Br J Pharmacol*. 2018;175(12):2219–2230. doi:10.1111/bph.13957
6. Wang H, Xu C. A novel progress: glial cells and inflammatory pain. *ACS Chem Neurosci*. 2022;13(3):288–295. doi:10.1021/acschemneuro.1c00607
7. Bereiter DA, Rahman M, Ahmed F, et al. Title: P2x7 receptor activation and estrogen status drive neuroinflammatory mechanisms in a rat model for dry eye. *Front Pharmacol*. 2022;13:827244. doi:10.3389/fphar.2022.827244
8. Sommer C, Leinders M, Üçeyler N. Inflammation in the pathophysiology of neuropathic pain. *Pain*. 2018;159(3):595–602. doi:10.1097/j.pain.0000000000001122
9. Jin T, Liu X, Li Y, et al. EA reduces ocular surface neuralgia in dry-eyed guinea pigs by inhibiting the trigeminal ganglion and spinal trigeminal nucleus caudalis P2X3R-PKC signaling pathway. *Curr Eye Res*. 2023;48(6):546–556. doi:10.1080/02713683.2023.2176886
10. Liu CY, Qin S, Gao WP, et al. 针刺对干眼兔泪腺中转化生长因子–β 1 表达的影响 [Effect of acupuncture on expression of transfer growth factor-β1 in lacrimal gland of rabbits with dry eye]. *Zhen Ci Yan Jiu*. 2020;45(9):726–730. Chinese. doi:10.13702/j.1000-0607.190977
11. Xin YY, Wang JX, Xu AJ. EA ameliorates neuroinflammation in animal models. *Acupunct Med*. 2022;40(5):474–483. doi:10.1177/09645284221076515
12. Pan S, Wang S, Xue X, et al. Multidimensional pain modulation by acupuncture analgesia: the reward effect of acupuncture on pain relief. *Evid Based Complement Alternat Med*. 2022;2022:3759181. doi:10.1155/2022/3759181
13. Sun SY, Yan QQ, Qiao LN, et al. EA alleviates pain responses and inflammation in collagen-induced arthritis rats via suppressing the TLR2/4-MyD88-NF- κ B signaling pathway. *Evid Based Complement Alternat Med*. 2023;2023:9050763. doi:10.1155/2023/9050763
14. Hsu HC, Hsieh CL, Lee KT, et al. EA reduces fibromyalgia pain by downregulating the TRPV1-pERK signalling pathway in the mouse brain. *Acupunct Med*. 2020;38(2):101–108. doi:10.1136/acupmed-2017-011395
15. Liu Y, Du J, Fang J, et al. EA inhibits the interaction between peripheral TRPV1 and P2X3 in rats with different pathological pain. *Physiol Res*. 2021;70(4):635–647. doi:10.33549/physiolres.934649
16. Fakih D, Zhao Z, Nicolle P, et al. Chronic dry eye induced corneal hypersensitivity, neuroinflammatory responses, and synaptic plasticity in the mouse trigeminal brainstem. *J Neuroinflammation*. 2019;16(1):268. doi:10.1186/s12974-019-1656-4
17. Li ZR. Experimental acupuncture and moxibustion; 2003.
18. Chen ZX, Li Y, Zhang XG, et al. Sham EA Methods in Randomized Controlled Trials. *Sci Rep*. 2017;7:40837. doi:10.1038/srep40837
19. Cordaro M, Siracusa R, D'Amico R, et al. Role of etanercept and infliximab on nociceptive changes induced by the experimental model of fibromyalgia. *Int J Mol Sci*. 2022;23:11. doi:10.3390/ijms23116139
20. Skrzypecki J, Huc T, Ciepiaszuk K, et al. Effect of TMAO, a gut-bacteria metabolite, on dry eye in a rat model. *Curr Eye Res*. 2019;44(6):651–656. doi:10.1080/02713683.2019.1574834

21. Bereiter DA, Rahman M, Thompson R, et al. TRPV1 and TRPM8 channels and nocifensive behavior in a rat model for dry eye. *Invest Ophthalmol Vis Sci*. 2018;59(8):3739–3746. doi:10.1167/iovs.18-24304
22. Fakih D, Migeon T, Moreau N, et al. Transient receptor potential channels: important players in ocular pain and dry eye disease. *Pharmaceutics*. 2022;14(9):1859. doi:10.3390/pharmaceutics14091859
23. Rahman M, Okamoto K, Thompson R, et al. Sensitization of trigeminal brainstem pathways in a model for tear deficient dry eye. *Pain*. 2015;156 (5):942–950. doi:10.1097/j.pain.0000000000000135
24. Meng ID, Barton ST, Mecum NE, et al. Corneal sensitivity following lacrimal gland excision in the rat. *Invest Ophthalmol Vis Sci*. 2015;56 (5):3347–3354. doi:10.1167/iovs.15-16717
25. Galor A, Levitt RC, Felix ER, et al. Neuropathic ocular pain: an important yet underevaluated feature of dry eye. *Eye*. 2015;29(3):301–312. doi:10.1038/eye.2014.263
26. Venkateswaran N, Hwang J, Rong AJ, et al. Periorbital botulinum toxin A improves photophobia and sensations of dryness in patients without migraine: case series of four patients. *Am J Ophthalmol Case Rep*. 2020;19:100809. doi:10.1016/j.ajoc.2020.100809
27. Zhao H, Alam A, Chen Q, et al. The role of microglia in the pathobiology of neuropathic pain development: what do we know? *Br J Anaesth*. 2017;118(4):504–516. doi:10.1093/bja/aex006
28. Kiguchi N, Kobayashi D, Saika F, et al. Inhibition of peripheral macrophages by nicotinic acetylcholine receptor agonists suppresses spinal microglial activation and neuropathic pain in mice with peripheral nerve injury. *J Neuroinflammation*. 2018;15(1):96. doi:10.1186/s12974-018-1133-5
29. Kikuchi K, Tagawa Y, Murata M, et al. Effects of mirogabalin on hyperalgesia and chronic ocular pain in tear-deficient dry-eye rats. *Invest Ophthalmol Vis Sci*. 2023;64(5):27. doi:10.1167/iovs.64.5.27
30. Yang Y, Zhang J, Gao Q, et al. Etanercept attenuates thermal and mechanical hyperalgesia induced by bone cancer. *Exp Ther Med*. 2017;13 (5):2565–2569. doi:10.3892/etm.2017.4260
31. Sperry MM, Yu YH, Kartha S, et al. Intra-articular etanercept attenuates pain and hypoxia from TMJ loading in the rat. *J Orthop Res*. 2020;38 (6):1316–1326. doi:10.1002/jor.24581
32. Ding N, Wei Q, Deng W, et al. EA alleviates inflammation of dry eye diseases by regulating the α 7nAChR/NF- κB signaling pathway. *Oxid Med Cell Longev*. 2021;2021:6673610. doi:10.1155/2021/6673610
33. Sun XY, Shen HX, Liu CY, et al. Acupuncture mitigates ocular surface inflammatory response via α7nAChR/NF-κB p65 signaling in dry eye Guinea pigs. *Zhen Ci Yan Jiu*. 2022;47(11):975–982. doi:10.13702/j.1000-0607.20220015
34. Xiang X, Wang S, Shao F, et al. EA stimulation alleviates CFA-induced inflammatory pain via suppressing P2X3 expression. *Int J Mol Sci*. 2019;20 (13):1. doi:10.3390/ijms20133248
35. Fei X, He X, Tai Z, et al. EA alleviates diabetic neuropathic pain in rats by suppressing P2X3 receptor expression in dorsal root ganglia. *Purinergic Signal*. 2020;16(4):491–502. doi:10.1007/s11302-020-09728-9
36. Krajewski JL. P2X3-containing receptors as targets for the treatment of chronic pain. *Neurotherapeutics*. 2020;17(3):826–838. doi:10.1007/s13311-020-00934-2
37. Kondo M, Shibuta I. Extracellular signal-regulated kinases (ERK) 1 and 2 as a key molecule in pain research. *J Oral Sci*. 2020;62(2):147–149. doi:10.2334/josnusd.19-0470
38. Guo SH, Lin JP, Huang LE, et al. Silencing of spinal Trpv1 attenuates neuropathic pain in rats by inhibiting CAMKII expression and ERK2 phosphorylation. *Sci Rep*. 2019;9(1):2769. doi:10.1038/s41598-019-39184-4
39. Xu R, Zhang YW, Gu Q, et al. Alteration of neural activity and neuroinflammatory factors in the insular cortex of mice with corneal neuropathic pain. *Genes Brain Behav*. 2023;22(2):e12842. doi:10.1111/gbb.12842
40. Sheng J, Liu S, Wang Y, et al. The link between depression and chronic pain: neural mechanisms in the brain. *Neural Plast*. 2017;2017:9724371. doi:10.1155/2017/9724371
41. Demartini C, Greco R, Francavilla M, et al. Modelling migraine-related features in the nitroglycerin animal model: trigeminal hyperalgesia is associated with affective status and motor behavior. *Physiol Behav*. 2022;256:113956. doi:10.1016/j.physbeh.2022.113956
42. Cao Y, Wang L, Lin LT, et al. Acupuncture attenuates cognitive deficits through α7nAChR mediated anti-inflammatory pathway in chronic cerebral hypoperfusion rats. *Life Sci*. 2021;266:118732. doi:10.1016/j.lfs.2020.118732
43. Tida JA, Catalão CHR, Garcia CAB, et al. Acupuncture at ST36 exerts neuroprotective effects via inhibition of reactive astrogliosis in infantile rats with hydrocephalus. *Acupunct Med*. 2018;36(6):386–393. doi:10.1136/acupmed-2017-011515
44. Huang S, Tang C, Sun S, et al. Protective effect of EA on neural myelin sheaths is mediated via promotion of oligodendrocyte proliferation and inhibition of oligodendrocyte death after compressed spinal cord injury. *Mol Neurobiol*. 2015;52(3):1870–1881. doi:10.1007/s12035-014-9022-0